Realize The Image Motion Self-Registration Based on TDI in Digital Domain

Shuping Tao, Xuyan Zhang, Wei Xu, and Hongsong Qu

***Abstract*—A novel image motion self-registration algorithm was proposed and realized to improve the effectiveness of Time-Delay-Integration image processing. Firstly, to overcome the defects of the on-chip accumulator, a CMOS camera with off-chip digital accumulator was designed. Compared to the traditional on-chip Time-Delay-Integration, the new off-chip digital Time-Delay-Integration cost none silicon area and can integrate signal processing easily. The novel algorithm was developed to work with this new off-chip digital Time-Delay-Integration. To assess the proposed algorithm, simulations and experiments were carried out. With the new algorithm, the cross-correlation similarity of the Time-Delay-Integration images improved from 0.9257 to 0.9587, even when the image motion mismatch rate is 0.1. Further experiments proved the effectiveness of the proposed algorithm when the image motion mismatch is existing. This algorithm is suitable for applications in remote sensing systems with characters of low-illumination and high scanning speed.**

***Index Terms*—CMOS, camera, image motion, in digital domain, Time-Delay-Integration**

I. INTRODUCTION

TIME-Delay-Integration (TDI) is a particular imaging mode used in cameras for decades. In general, the signal is increased by a factor M for an M-stage TDI, and the signal-to-noise ratio (SNR) is increased by $\sqrt{M}$ times. Due to this characteristic, TDI camera is widely used in line scan applications where a line-scan system is required under low illumination condition and at high scanning speed. A well-known application is push-broom imaging for earth observation from satellite or aircraft.

TDI can be easily applied on the charge-coupled device (CCD), because it allows noiseless accumulation of charge packets synchronously with the moving image. However, the TDI CCD requires a high-power operation, and it is difficult to control. A typical CCD camera consumes no less than 10W, while the complementary metal-oxide-semiconductor (CMOS) cameras typically consume only 3W. In addition, CCD cameras not only involve analog signal processing, but also require additional video processors, but CMOS cameras are completely digital signal processing with simple control.

The CMOS technology is getting attention because it overcomes several defects of CCD and has features such as low-power, low-cost, and high-integration[1]. Since charge cannot be stored in CMOS for a long time, there are usually two ways to achieve TDI (1) accumulated in analog domain and (2) accumulated in digital domain. In analog domain, the signals could be the type of voltage or current; in digital domain, the signals output from the pixels are quantized firstly, and then accumulated as the type of digital signals. In [2], several CMOS TDI image sensors with analog accumulator were summarized, but the most significant drawback of these methods with analog accumulator is the cost of silicon area. In [3], an addition in digital domain reached in a ramp analog-to-digital converter (ADC) with a local counter was presented. In [4], a 128-stage CMOS TDI image sensors with on-chip digital accumulator was presented, and an on-chip column cyclic ADC was used to reduce the silicon area. Although the on-chip digital accumulation becomes simpler than that in analog domain, the on-chip circuitry still costs some areas. Moreover, the fixed on-chip accumulator architecture forces the scene to impinge successively on each pixel of the given corresponding column.

Although the accumulation in charge domain is difficult for CMOS sensor, several reports on TDI CMOS image sensor based on pipelined charge transfer architecture were presented recently. In [5]–[7], noise free pipelined charge transfer was achieved, where CCD structure were realized through standard CMOS technology, but this structure highly relies on foundry's technology and still suffers from low charge transfer efficiency. In [8], low noise pipelined signal accumulation are achieved by the PCT-pixel based on CTIA technique, but the TDI stage is limited and the fill factor is low.

To overcome the defects of the on-chip accumulator, CMOS TDI camera with an off-chip digital accumulator is proposed in [9]-[11]. The digital TDI is implemented in external programmable devices, such as the Field Programmable Gate Array (FPGA). Compared to the on-chip TDI, the off-chip digital TDI costs none silicon areas, and it is easy to integrate signal processing so that some new function can be further developed based on the off-chip digital TDI.

Due to the pixel signals at different exposure times are added

This work was supported in part by the National Natural Science Foundation of China under Grant 61805244, in part by the Youth Science Foundation of Jilin Province, China under Grant 20180520193JH, and in part by the Key Technological Research Projects of Jilin Province, China, under Grant 20190303094SF. (Corresponding author: Shuping Tao.)

The authors are with Changchun Institute of Optics, fine Mechanics and Physics, Chinese Academy of Sciences, Changchun, Jilin 130033, China. (e-mail: taoshuping11@sina.com; zhangxuyan138@163.com; xwciomp@126.com; quhongsong@aliyun.com.)

together in TDI, the key for clear imaging is that each pixel acquires exactly the same object. However, the orbit parameters and satellite's attitude change constantly, especially in the agile imaging mode, the image scene moves relative to the detector with an unfixed velocity. In such case, a precise image motion compensation is necessary. Otherwise, the TDI image will blur seriously if the image motion mismatch exists.

Currently, there are three methods to compensate for the image motion, optical, mechanical, and electronic method[12]-[14]. The optical method is generally used for aerial cameras, which reduces the image motion mismatch by changing the direction of light with another specific optical system[15].The mechanical method is commonly used to adjust the deviant angle, in which the focal plane is moved in whole or slice when exposure to keep consistent with the image scene moving[16]. The electronic method adjusts the transfer time through programming to match the image motion along track[17]. However, the optical and mechanical methods rely on high-precision optical systems or mechanical structures, which increase the complexity and cost, but lower the reliability; while the electronic method can only compensate the mismatch along the track, and its compensable range is limited. Therefore, design a simple but precise method for image motion compensation is an urgent need.

In our previous work[9,10], an off-chip digital CMOS TDI camera was presented, on the foundation of this, an image motion self-registration algorithm is further developed in this paper. In the proposed algorithm, the outputs of pixels are first corrected, and then the corresponding correction results are added together to achieve the whole TDI process. Compared to TDI CCD and CMOS TDI with the on-chip accumulator, the proposed method implements TDI not constrained by the chip and makes the image motion compensation easier.

In section 2, the CMOS TDI camera and the off-chip TDI algorithm in digital domain are described. In section 3 introduced the image motion self-registration algorithm based on TDI in digital domain. In section 4, the new algorithm's performance on synthetic images as well as the imaging experiment is accessed. Finally, a brief conclusion is drawn in section 5.

II. The Off-Chip TDI In Digital domain

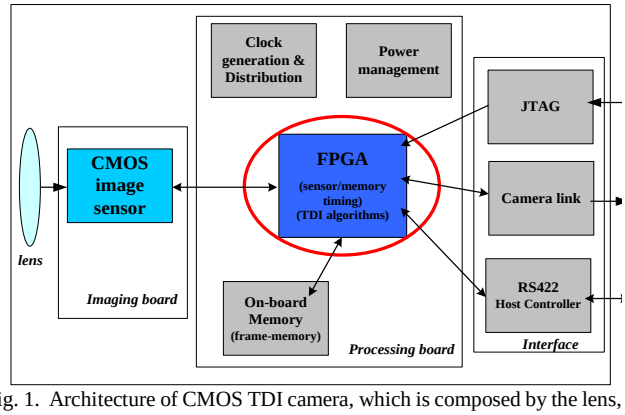

Fig. 1. Architecture of CMOS TDI camera, which is composed by the lens, imaging board, processing board, and an interface.

A. Architecture of the CMOS TDI Camera

Fig. 1 shows the architecture of the designed CMOS TDI camera, which is composed by the lens, imaging board, processing board, and an interface.

The main component of the imaging board is CMOS sensor. FPGA is the control center of the system. All the other chips operate under FPGA's control, such as CMOS sensor, memory and interfaces. Besides, the digital addition and image motion self-registration algorithm are implemented in FPGA. As shown in Fig.1, the proposed CMOS TDI camera needs none additional hardware compared to the regular CMOS camera without TDI function. So, the off-chip TDI can be reconstructed conveniently.

B. The TDI Algorithm in Digital Domain

Different from the TDI in analog domain, the TDI in digital domain has the signal's accumulation happened after the sensor's ADC. In the off-chip TDI imaging, the parameters such as line time, frame period, invalid time and TDI stages are calculated firstly to meet the demands of TDI. Then the CMOS driving timing is generated under the corresponding parameters. The CMOS outputs digital signal generated by a single exposure continuously, and then the digital signals of multi-exposures on the same objects synchronously with the optical scanning are added in the work of FPGA with memory. Finally, the integration signal is output.

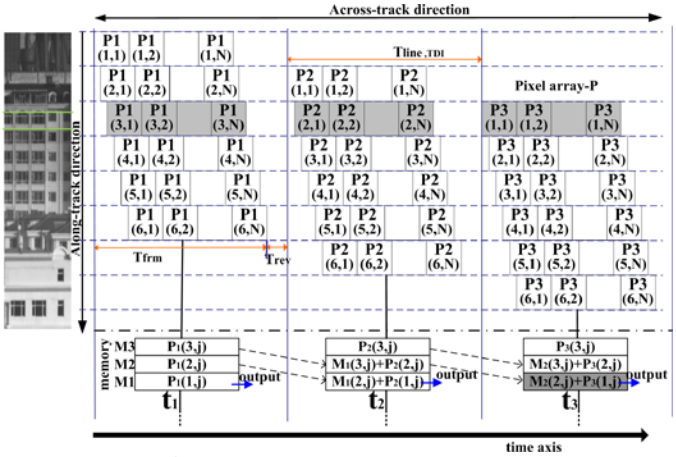

Fig. 2. Timing of TDI in digital domain with 3-stage, which is progressive pixel accumulation.

Taking the TDI with 3-stage as an example, the working principle of the digital TDI algorithm which is progressive pixel accumulation is shown in Fig. 2. In Fig.2, the drift angle is zero, and the motion direction is called "along-track," while its orthogonal direction is called "across-track". When performing push-broom imaging, the speed of the image in along-track direction is 1-pixel and the sensor outputs one frame image per line time ($T_{\text{line},TDI}$). Here use $P_k(i,j)$ to represent the i-th row, the j-th column pixel in the k-th frame image. At time t1, the CMOS sensor outputs the frist frame image P_1, and its first 3-rows of pixels are written into memory M1 to M3 respectively. After one line time, the sensor moves by 1-pixel in along-track direction, and P_2 is output at time t2. The first row of pixels in P_2 photos on the same object as the second row of

This article has been accepted for publication in a future issue of this journal, but has not been fully edited. Content may change prior to final publication. Citation information: DOI 10.1109/JSEN.2019.2935112, IEEE Sensors Journal

pixels in P_1, and the second row of pixels in P_2 photos on the same object as the third row of pixels in P_1, so two rows of pixels with the same object scene are added and then restored in M1 and M2 respectively. And then the third row of pixels in P_2 is written in M3. Similarly, at time t3, the signal stored in M1 is the accumulation of the first row in P_3, the second row in P_2 and the third row in P_1, and it is output as the TDI result:

$$N_3(1,j)=P_3(1,j)+P_2(2,j)+P_1(3,j),1\le j\le n_{pixels} \tag{1}$$

Where n_{pixels} is the number of pixels per row, $N_k(1,j)$ is the j-th column integration pixel in the k-th line time.

The principle remains the same as the integration stage changes. Therefore, we can derive the equation of TDI algorithm in digital domain:

$$\begin{aligned} N_k(1,j)=&P_k(1,j)+P_{k-1}(2,j)+\cdots \\ &+P_{k-(M-2)}(M-1,j)+P_{k-(M-1)}(M,j), \\ &1\le j\le n_{pixels} \end{aligned} \tag{2}$$

Where M is the stage, k is the k-th frame or k-th line time, $P_k(i,j)$ denotes the pixel with i-row and j-column in the k-th frame.

To avoid the overflow saturation distortion, take the maximum quantization value when the accumulation exceeds the maximum value:

$$N_k'(1,j)=\begin{cases} N_k(1,j), N_k(1,j)\le 2^n-1 \\ 2^n-1, N_k(1,j)>2^n-1 \end{cases},1\le j\le n_{pixels} \tag{3}$$

Where n is the quantization bits.

However, the parameters such as line time, windowing lines, reversing time and TDI stages need to be calculated firstly to meet the demands of TDI. As shown in (4), TDI line time is defined as a time that image moves one pixel, and each line time consists of valid time(identified as T_{frm} in Fig.2) and reversing time(identified as T_{rev} in Fig.2). The valid time is also the frame period of the CMOS sensor to generate one frame, in which the CMOS sensor resets, exposures and readouts. In reversing time, the sensor has no action, but it is needed to adjust the line time continuously.

$$T_{line,TDI}=\frac{a}{V_p}=T_{frm}+T_{rev} \tag{4}$$

$$T_{frm}=\left(T_{rb}+n_{pixels}\cdot\frac{1}{f_s}\right)\cdot n_{lines} \tag{5}$$

$$0\le T_{rev}<T_{rb}+n_{pixels}\cdot\frac{1}{f_s} \tag{6}$$

Where a is the pixel size, V_p is the image motion velocity which can be derived from the image plane position equation obtained by homogeneous coordinate transformation[12], T_{rb} is the row blank time which is needed for CMOS sensor before the image read-out, and f_s is the sampling frequency. In our designed TDI algorithm, T_{rev} satisfies the condition of (6). Based on the above analysis, we can further derive the calculation equations of the number of windowing lines (n_{lines}) and T_{rev} as:

$$n_{lines}=\frac{\frac{a}{V_p}-T_{rev}}{T_{rb}+n_{pixels}\cdot\frac{1}{f_s}} \tag{7}$$

$$T_{rev}=\frac{a}{V_p}-\left\{\left(T_{rb}+\frac{n_{pixels}}{f_s}\right)\cdot rem\left(\frac{a}{V_p}\Big/\left(T_{rb}+\frac{n_{pixels}}{f_s}\right)\right)\right\} \tag{8}$$

When the line time changes, both n_{lines} and T_{rev} can be adjusted to match the image motion in the proposed algorithm. In addition, the TDI stage is continuously adjustable within a range of 1 to n_{lines}, while on-chip TDI can adjust stage by several steps.

III. The Image Motion Self-Registration TDI Algorithm

Firstly, two coordinate systems are defined for analysis. The camera motion coordinate system is represented by UO_1V, where U-axis is the along-track direction and V-axis is the across-track direction. Here, the camera's motion direction is called "along-track", while its orthogonal direction is called "across-track". The image coordinate system is represented by XO_2Y, where X-axis corresponds to the rows of the sensor and Y-axis corresponds to the columns of the sensor. In Fig.3, $P_k(i,j)$ is the direct output signal of CMOS sensor in the k-th frame, and $O_M(i,j)$ is the integration output with M-stage in digital domain. V_{P1} and V_{P2} represent the image motion velocities along X-axis and Y-axis respectively, and the drift angle can be gotten as $\theta=\arctan(V_{P2}/V_{P1})$. When the drift angle is zero, the two coordinate systems are parallel.

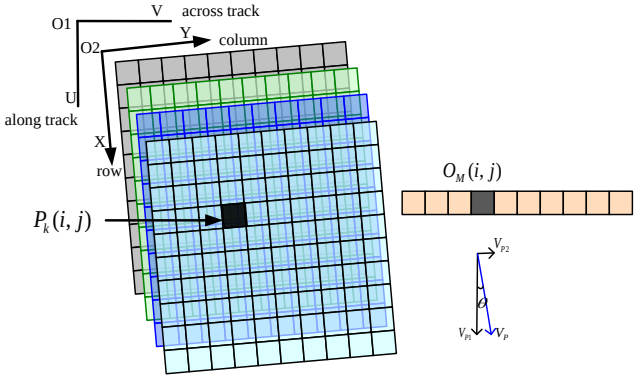

Fig. 3. The coordinates of TDI in digital domain for push-broom imaging. UO_1V represents the camera motion coordinate system and XO_2Y represents the image coordinate system.

Due to the fixed on-chip circuit structure in TDI CCD or TDI CMOS sensors, clear imaging does not allow image motion mismatch. However, the image motion deviation often exits, as shown in Fig.4. In this case the TDI image will blur, and the higher the stage the more blurred the image. In order to solve this problem, one correction algorithm for the pixel array is designed before the digital addition in this paper.

This article has been accepted for publication in a future issue of this journal, but has not been fully edited. Content may change prior to final publication. Citation information: DOI 10.1109/JSEN.2019.2935112, IEEE Sensors Journal

As shown in Fig.4, Δx and Δy present the deviation amount in the row and column direction respectively. They can be derived from (9). And then the number of pixels corresponding to the deviation is calculated as (10).

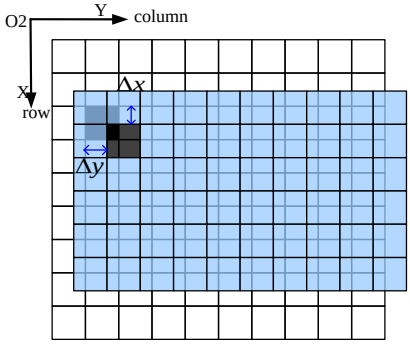

Fig. 4. The pixel deviation. Δx and Δy present the deviation amount in the row and column direction respectively.

$$\begin{aligned}\Delta x &= \int_{t_0}^{t_0+kT_{line,TDI}} V_{p1}dt - ka \\ \Delta y &= \int_{t_0}^{t_0+kT_{line,TDI}} V_{p2}dt\end{aligned} \tag{9}$$

$$\begin{aligned}\Delta m(k) &= \frac{\int_{t_0}^{t_0+kT_{line,TDI}} V_{p1}dt - ka}{a} \\ \Delta n(k) &= \frac{\int_{t_0}^{t_0+kT_{line,TDI}} V_{p2}dt}{a}\end{aligned} \tag{10}$$

Where Δm and Δn represent the number of pixels corresponding to the image motion deviation in the row and column direction respectively. The grayscale of the pixel is determined by the number of photoelectric charges, and the number of photoelectric charges is proportional to the photosensitive area. So considering each pixel's contribution to the grayscale, the modified pixel array can be gotten as follows.

$$P_k'(i,j) = \begin{bmatrix} P_k(i,j) \\ P_k(i+\delta,j) \\ P_k(i,j+\lambda) \\ P_k(i+\delta,j+\lambda) \end{bmatrix}^T \cdot \begin{bmatrix} 1 & -1 & -1 & 1 \\ -1 & 1 & 0 & 0 \\ -1 & 0 & 1 & 0 \\ 1 & 0 & 0 & 0 \end{bmatrix} \cdot \begin{bmatrix} \Delta m''(k)\Delta n''(k) \\ \Delta m''(k) \\ \Delta n''(k) \\ 1 \end{bmatrix} \tag{11}$$

$$\begin{aligned}\Delta m''(k) &= \left|\Delta m(k) - \Delta m'(k)\right| \\ \Delta n''(k) &= \left|\Delta n(k) - \Delta n'(k)\right|\end{aligned} \tag{12}$$

$$\begin{aligned}\Delta m'(k) &= round\left(\frac{\int_{t_0}^{t_0+kT_{line,TDI}} V_{p1}dt - ka}{a}\right) \\ \Delta n'(k) &= round\left(\frac{\int_{t_0}^{t_0+kT_{line,TDI}} V_{p2}dt}{a}\right)\end{aligned} \tag{13}$$

$$\delta = \begin{cases} 1, \Delta m(k) < \Delta m'(k) \\ -1, others \end{cases} \tag{14}$$

$$\lambda = \begin{cases} 1, \Delta n(k) < \Delta n'(k) \\ -1, others \end{cases} \tag{15}$$

In order to make the modified pixel closest to the real value, the nearest integer is getting rounded up or down, and different pixels are interpolated. In (13), $\Delta m'(k)$ and $\Delta n'(k)$ are the nearest integer to the number of rows and columns of deviations in the k-th frame. When rounded up, the current pixel and its adjacent next pixel are used for interpolation calculation. When rounded down, the current pixel and its adjacent previous pixel are used for interpolation calculation. Here δ represents the symbol of the two numbers after and before the rounding in the row direction, and λ represents the symbol of the two numbers after and before the rounding in the column direction. The proportion of each pixel in interpolation is determined by the non-integer pixel deviation coefficients in the row and column direction, where $\Delta m''(k)$ is the non-integer pixel deviation coefficients in the row direction and $\Delta n''(k)$ is the non-integer pixel deviation coefficients in the column direction. For the boundary pixel, when it coincides with the previous frame image, the previous frame image and the current frame image are interpolated together. When there is no coincidence, the nearest frame pixel value of the current frame is taken as the modified boundary pixel.

Based on the modified pixel array, we can get the self-registration integration image with M-stage as (16):

$$O_M(i,j) = P_k'(i,j) + \sum_{l=1}^{M-1} P_{k-l}'(i+\Delta m'(k-l), j+\Delta n'(k-l)) \tag{16}$$

When the image motion in the row direction is exactly 1-pixel and the image motion in the column direction is 0, the image motion mismatch is 0, and the proposed algorithm can obtain a clear image without any quality loss. In addition, as long as the image motion mismatch is less than 0.5-pixel in one line time, the proposed algorithm can obtain a clear integral image with uniform gray level. When the mismatch is greater than 0.5, because the algorithm adopts the idea of aligning the accumulation, the image will still not be aliased, but the gradation unevenness will occur and further correction is needed. In the following description, the algorithm herein only considers the case where the image motion mismatch is less than 0.5.

IV. Experiment Results And Analysis

Fig. 5. Simulation sample.

To validate the proposed algorithm, one remote sensing image is chosen as an example, as shown in Fig.5. To simulate adequately, the image motion mismatch amounts set to be 0.1(along the track) and 0.0875(across the track) respectively.

This article has been accepted for publication in a future issue of this journal, but has not been fully edited. Content may change prior to final publication. Citation information: DOI 10.1109/JSEN.2019.2935112, IEEE Sensors Journal

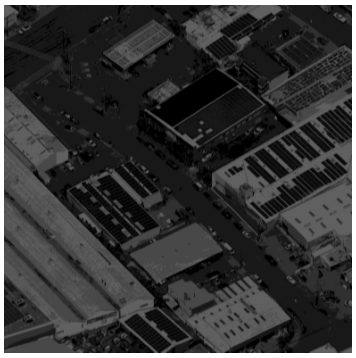

(a)24-stage

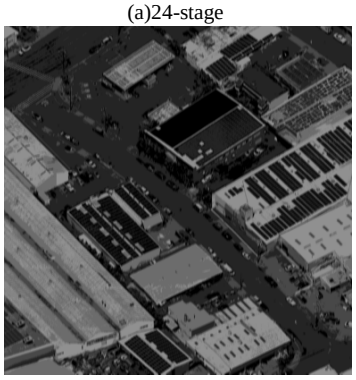

(b)36-stage

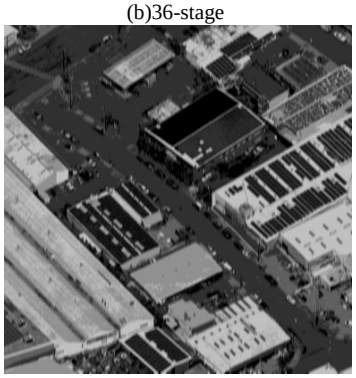

(c)48-stage

Fig. 6. The images gotten by the proposed algorithm, where the image motion mismatch amount is 0.1(along the track).

(a)24-stage

(b)36-stage

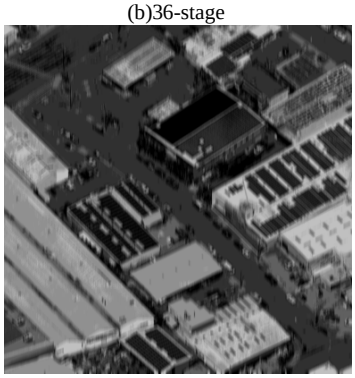

(c)48-stage

Fig. 7. The images gotten by the traditional method, where the image motion mismatch amount is 0.1(along the track).

In each mismatch amount, the TDI images are generated with 24, 36 and 48-stage. In addition, the TDI images by a traditional method which uses the same principle as TDI CCD are generated for comparison. The simulation results by the proposed algorithm are shown in Fig.6 and Fig.7, and the simulation results by the traditional method are shown in Fig.8 and Fig.9.

The results show that the images generated by the proposed algorithm are clearer than those of the traditional method if the mismatch amount and the integration stage are all the same. To compare two methods' performance, the cross-correlation similarity measure (σ)of these images are calculated, as shown in table 1. The σ is defined as:

$$\sigma = \frac{\sum_{m=1}^{M}\sum_{n=1}^{N}[S^{i,j}(m,n)\times T(m,n)]}{\sqrt{\sum_{m=1}^{M}\sum_{n=1}^{N}[S^{i,j}(m,n)]^2}\times\sqrt{\sum_{m=1}^{M}\sum_{n=1}^{N}[T(m,n)]^2}} \tag{17}$$

Where $T(m,n)$ is the original sample, and $S(m,n)$ is the image to be evaluated.

TABLE I
THE EVALUATION RESULTS OF THE IMAGES GOTTEN BY TWO METHODS

the rate of the image motion mismatch	integration stage	cross-correlation similarity measure (σ)	
		the proposed method	the traditional method
0.1 (along the track)	24-stage	0.976148	0.946467
	36-stage	0.965939	0.934603
	48-stage	0.958720	0.925674
0.0875 (across the track)	24-stage	0.983566	0.955185
	36-stage	0.974985	0.944952
	48-stage	0.967717	0.936680

The smaller the distortion and quality degradation, the higher the σ compared to the sample image. In table 1, the results show that the images generated by two methods both degrade

This article has been accepted for publication in a future issue of this journal, but has not been fully edited. Content may change prior to final publication. Citation information: DOI 10.1109/JSEN.2019.2935112, IEEE Sensors Journal

(a)24-stage

(b)36-stage

(c)48-stage

Fig. 8. The images gotten by the proposed algorithm, where the image motion mismatch amount is 0.0875(across the track).

(a)24-stage

(b)36-stage

(c)48-stage

Fig. 9. The images gotten by the traditional method, where the image motion mismatch amount is 0.0875(across the track).

as the integration stage increases, but the images with the proposed method degrade much more slowly than those of TDI CCD. Furthermore, a cross-correlation similarity measure higher than 0.9587 can be obtained with the proposed method, while that of TDI CCD is only 0.9257. Obviously, the proposed method performs better in the imaging quality, that is, it is with more details, especially when the image motion mismatch exists.

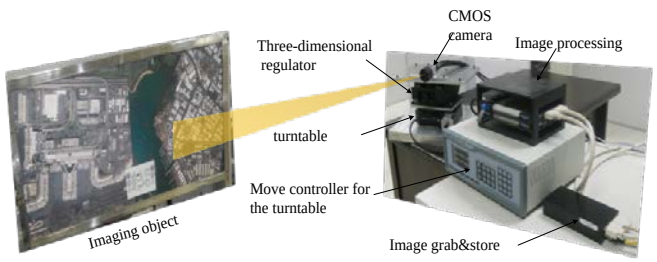

Fig. 10. The imaging experiment.

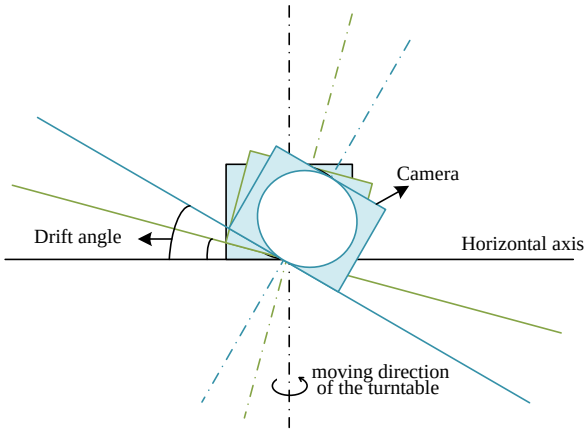

Fig. 11. The schematic diagram of drift angle.

This article has been accepted for publication in a future issue of this journal, but has not been fully edited. Content may change prior to final publication. Citation information: DOI 10.1109/JSEN.2019.2935112, IEEE Sensors Journal

Then verification was implemented on imaging experiments, the experiment system is shown in Fig.10. The CMOS camera is mounted vertically on the three-dimensional regulator, and then the whole is fixed on the horizontal turntable. Under the motion of the horizontal turntable, the camera acquires successive multi-frame images of the imaging object. And different drift angles can be obtained by adjusting the 3D regulator, as shown in Fig. 11. After the algorithm processing in the imaging processing board, the TDI image is obtained. The imaging parameters selected for the experiment are shown in table 2. When the drift angle is 0, the sensor's column is just perpendicular to the horizontal turntable, and the image motion can be perfectly matched by appropriately setting the horizontal turntable speed and the frame period.

Then keep the turntable speed and frame period unchanged, as long as the drift angle is not 0, the image motion mismatch occurs in both the row and column directions, and the larger the drift angle, the larger the row and column image motion mismatch. Because the applicable condition of the algorithm is that the image motion mismatch rates in both the row and column directions do not exceed 0.5, the maximum drift angle allowed by the experiment is 30 degrees. Therefore, in this range, three different drift angles are set to verify the algorithm.

TABLE 2
THE IMAGING PARMETERS OF THE EXPERIMENT

Pixel size	5.5um
Focal length	50mm
Imaging distance	10m
Frame period	0.128ms
Horizontal turntable speed	0.859375rad/s
Integration stage	48

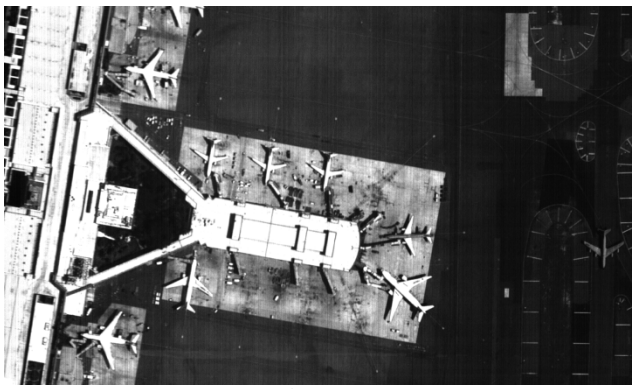

(a) the drift angle is 8.12°

(b) the drift angle is 11.31°

(c) the drift angle is 16.16°

Fig.12. The imaging results of the proposed method with 48-stage at different drift angles

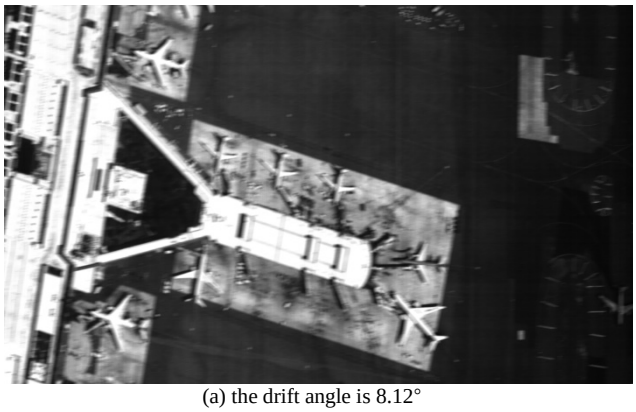

(a) the drift angle is 8.12°

(b) the drift angle is 11.31°

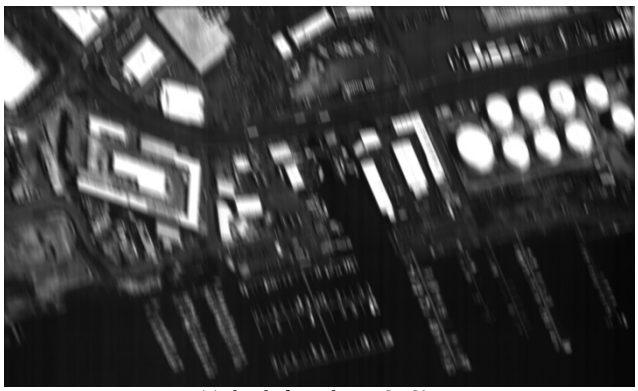

(c) the drift angle is 16.16°

Fig.13. The imaging results of the traditional method with 48-stage at different drift angles

This article has been accepted for publication in a future issue of this journal, but has not been fully edited. Content may change prior to final publication. Citation information: DOI 10.1109/JSEN.2019.2935112, IEEE Sensors Journal

TABLE 3
THE EVALUATION RESULTS OF THE IMAGES IN THE IMAGING EXPERIMENT

the drift angle	the proposed method			the traditional method		
evaluation indicators	8.12°	11.31°	16.16°	8.12°	11.31°	16.16°
definition	77.83	66.78	52.83	47.09	42.91	35.66
contrast	78.35	74.94	69.00	72.50	67.44	65.44
gradient	15.58	14.64	10.93	9.42	6.25	4.66
entropy	5.01	4.94	4.89	4.88	4.73	4.61
power spectrum	25.08	24.94	24.29	24.98	24.71	24.16
detail energy	142.50	113.67	86.77	97.88	68.95	62.73
cross-correlation similarity measure (σ)	0.74	0.70	0.63	0.58	0.43	0.26

The imaging results of the proposed method are shown in Fig.12, while those of the traditional method are shown in Fig.13. Obviously, as the drift angle gets larger, the image quality gets worse and worse. However, the imaging results of the proposed method are better than those of the traditional method in any of the three different drift angles. In addition, when the drift angle is present, the images generated by the traditional method have serious geometrical distortions, but the geometrical distortions of the images generated by the proposed method are almost eliminated. Comparing Fig.12 and Fig.13, it is clear that the image obtained by the proposed method still keeps many details even when the drift angle reaches to 16.16°, while the image generated by the traditional method has become very blurry.

To further quantify the comparison, several objective image evaluation indicators and the cross-correlation similarity are calculated for the above images, as shown in table 3. When measuring the cross-correlation similarity, the original samples are acquired using the camera area array imaging mode. With the increase of the drift angle, the traditional method changes the image shape to be serious except for the imaging blur, which has a great influence on the cross-correlation similarity measure. Therefore, the similarity of Fig.13(c) drops sharply, only 0.26. However, the similarity of the proposed algorithm can still be kept at 0.63 under the same conditions. The proposed algorithm not only improves the imaging blur because of the image motion self-registration technology, but also can control the image without sharp deformation in the case of large image motion mismatch, so it has a higher cross-correlation similarity and shows significant improvement especially for conditions with larger drift angle. In table 3, the results show that the proposed method yields higher objective evaluation indicators and cross-correlation similarity than its counterpart. This result proves that the proposed method performs better in the imaging quality and is more effective than the traditional method.

In the proposed algorithm, as long as the image motion mismatch rate does not exceed 0.5, the registered pixels to be accumulated can be obtained by correction algorithm, so that clear integration images can be obtained. However, the condition of clear imaging of the traditional TDI algorithm is that the total image motion mismatch is less than 1/3 of one pixel. When the integration stage is 48, the allowed image motion mismatch rate is only 0.0069. Obviously, the proposed algorithm not only relaxes the requirements of clear imaging, but also obtains clearer images and better quality under the same image motion mismatch rate due to the image motion self-registration technique.

V. CONCLUSION

This work proposed a simple but effective image motion self-registration TDI algorithm, which is designed to meets the needs of line scanning cameras. Compared to the conventional image motion compensation method, the proposed algorithm (based on off-chip TDI in digital domain) has several advantages, such as simple optical and machine structures and wider adjustable range of image motion match. The proposed algorithm has been validated via series of simulations and imaging experiments. The results show that the integration images using the proposed algorithm are clearer than the one generated by the traditional method. The new algorithm can provide high quality image with less distortion and degradation even when the image motion mismatch rate is high (up to 0.1). In general, the proposed algorithm performs better in the imaging quality than the traditional method in all simulations and experiments.

ACKNOWLEDGMENT

The authors would like to acknowledge the team of remote sensing imaging for their active involvements in the project. The authors would also like to deeply thank X. Y. Zhao, a Ph.D. at the University of Toronto, whose advice and help in the English writing are invaluable.

REFERENCES

[1] G. Lepage, D. Dantès, and W. Diels, “CMOS long linear array for space application,” in Proc. SPIE-IS&T Electronic Imaging, 2006, pp.299-302.
[2] K. M. Nie, S. Y. Yao, and J. T. Xu, “A 128-Stage Analog Accumulator for CMOS TDI Image Sensor,” IEEE TRANSACTIONS ON CIRCUITS AND SYSTEMS, vol. 61, no. 7, pp. 1952-1961, 2014.

[3] G. Lepage, J. Bogaerts, and G. Meynants, "Time-Delay-Integration Architectures in CMOS Image Sensors," IEEE Transactions on Electron Devices, vol. 56, pp. 2524-2533, 2009.
[4] K. M. Nie, J. T. Xu, and ZH. Y. Gao, "A 128-Stage CMOS TDI image sensor with on-chip digital accumulator," IEEE SENSORS JOURNAL, vol. 16, no. 5, pp. 1319-1324, 2016.
[5] F. Mayer, H Bugnet, S Pesenti, et al., "First measurements of true charge transfer TDI (Time Delay Integration) using a standard CMOS technology," in Proc. International Conference on Space Optics, 2012, pp.10564N.
[6] A. Ercan, L. Haspeslagh, K. De Munck, K. Minoglou, A. Lauwers, and P. De Moor, "Prototype TDI sensors in embedded CCD in CMOS technology," in Proc. Int. Image Sensor Workshop, 2013, pp. 1–4.
[7] F. Mayer et al., "CMOS charge transfer TDI with front side enhanced quantum efficiency," in Proc. Int. Image Sensor Workshop, 2015, pp. 1–4.
[8] J. T. Xu, X. L. Shi, K. M. Nie, and Z. Y. Gao, "A Global Shutter High Speed TDI CMOS Image Sensor With Pipelined Charge Transfer Pixel," IEEE SENSORS JOURNAL, vol. 18, no. 7, pp. 2729-2736, 2018.
[9] SH. P. Tao, G. Jin, and H. S. Qu, et al. "Design and Analysis of CMOS Camera Based on Time Delay and Integration in Digital Domain to Realize Spatial High-Resolution Imaging," ACTA OPTICA SINICA, vol. 32, pp. 0411001, 2012.
[10] SH. P. Tao and G. Jin, "Influence Analysis on the Rolling Shutter for Time Delay and Integration in Digital Domain," ACTA OPTICA SINICA, vol. 35, pp. 0311001, 2015.
[11] E. Bodenstorfer, J. Fürtler, J. Brodersen, K. J. Mayer, C. Eckel, K. Gravogl, and H. Nachtnebel, "High-speed Line-Scan Camera with Digital Time Delay Integration," Proc. of SPIE-IS&T Electronic Imaging, SPIE Vol. 6496, 649601, 2007.
[12] J. Q. Wang, "Space Optical Remote Sensor Image Motion Velocity Vector Computational Model, Error Budget and Synthesis" Chinese Optics Letters, vol. 3, pp. 414-417, 2005.
[13] K. Janschek, V. Tchernykh, and S. Dyblenko, "Integrated camera motion compensation by real time image motion tracking and image deconvolution," in Proc. IEEE/ASME International Conference on Advanced Intelligent Mechatronics, California, USA, 2005, pp. 628-632.
[14] B.M. Miller and E.Ya. Rubinovich, "Image Motion Compensation at Charge-coupled Device Photographing in Delay-Integration Mode," Automation and Remote Control,. vol. 68, pp. 564-571, 2007.
[15] P. Jia, B. Zhang, and H. Sun, "Restoration of Motion-Blurred Aerial Image," Opt. Precision Eng, vol. 14, pp. 697-703, 2006.
[16] X. B. Yang, X. J. He, and L. Zhang, et al. "Effect and Simulation of the Deviant Angle Error on TDI CCD Cameras Image," Opto-Eletronic Engineering, vol. 35, pp. 45-56, 2008.
[17] X. J. He, X. B. Yang, and G. Jin, et al. "Imaging Model and Image Recovering Algorithms ofSpaceborne Camera in the End ofOrbit Life," Acta Geodaeticaet Cartographica Sinica, vol. 39, pp. 579-584, 2010.

Shuping Tao received the B.S. degree in communication engineering from Sichuan University in 2008, where she received the Ph.D. degree in optics engineering from University of Chinese Academy of Sciences in 2013. Since 2013, she has been with the Changchun Institute of Optics, Fine Mechanics and Physics, Chinese Academy of Sciences, Changchun, China, where she is currently an Associate Research Fellow. Her research interests are in digital circuit design and image signal processing.

Xuyan Zhang received the B.S. degree from Changchun University of Technology in 2008, and the M.S. degree in optics engineering from Harbin Institute of Technology in 2010.

After graduation, he worked at the Changchun Institute of Optics, Fine Mechanics and Physics, Chinese Academy of Sciences, Changchun, China. Now, he is an Associate Research Fellow. His current research interests include the Photoelectric imaging technology.

Wei Xu received the B.S. degree in mechanical and electronic engineering from Jilin University, Changchun, China, in 2003, and the Ph.D. degree in mechanical and electronic engineering from the Changchun Institute of Optics, Fine Mechanics and Physics, Chinese Academy of Sciences, Changchun, China, in 2008.

After graduation, he worked at the Changchun Institute of Optics, Fine Mechanics and Physics, Chinese Academy of Sciences, Changchun, China. Now, he is a Research Fellow and a Doctoral Supervisor. His current research interests include the integration technology of satellites and payloads and the high reliable electronic systems for aerospace.

Hongsong Qu received the B.S. degree in mechanical and electronic engineering from Jilin University, Changchun, China, in 2003, and the Ph.D. degree in mechanical and electronic engineering from the Changchun Institute of Optics, Fine Mechanics and Physics, Chinese Academy of Sciences, Changchun, China, in 2008. He stayed and worked at the Changchun Institute of Optics, Fine Mechanics and Physics, Chinese Academy of Sciences, Changchun, China. And now he is a Research Fellow. His current research interest lies in the space-borne camera system technology.